ISSN 1590-8844
International Journal of Mechanics and Control, Vol. 17, No. 01, 2016

DESIGN AND TESTS OF TEXTILE PNEUMATIC MUSCLES FOR ACTIVE SUITS

G. Belforte* E. Bonisoli** G. Eula* A. Ivanov* S. Sirolli*

*Dept. of Mechanical and Aerospace Engineering

**Dept. of Management and Production Engineering

Politecnico di Torino – C.so Duca degli Abruzzi, 24 – 10129 Torino

ABSTRACT

This paper describes the design and test of some textile pneumatic muscles prototypes. Tests were carried out on materials, geometries and some numerical models constructed for a better characterization of these devices. The results are interesting and provide ideas for further research in applications such as active clothing where the pneumatic muscle, integrated in a T-shirt, allows the wearer to perform rehabilitation exercises.

Keywords: textile pneumatic muscles for active suits; active clothing with pneumatic muscles; textile pneumatic muscles numerical models.

1 INTRODUCTION

Pneumatic Artificial Muscles or PAMs are used as actuators which can simulate human muscle for rehabilitation purposes or to assist the movement of injured limbs [1, 2].
They simulates the behaviour of a human muscle, contracting thanks to the pressure of the fluid in its interior to generate a traction force at its ends.
The structure typically consists of a rubber or textile material, generally anisotropic, rigid in one direction and elastic in the orthogonal direction to permit axial deformation.
PMAs have been most commonly used in areas such as medical, industrial and entertainment robotics [3-10].
Soft materials are essential to the mechanical design of innovative actuators. The soft components provide numerous advantages. They conform to surfaces, distribute stress over a larger volume, and increase contact time, thereby lowering the maximum impact force [11].
If the fabric is not impermeable, or if the seams of the muscle assembly can leak, the outer fabric contains an interior latex tube which is impermeable to the supplied fluid [12-14].

Contact author: Gabriella Eula

Email: gabriella.eula@polito.it

The two concentric tubes are connected at their ends to fittings whereby the load is moved. Like human muscles, PAMs also operate in antagonistic pairs, since they can only generate traction forces and therefore movements in just one direction.
One innovative application for pneumatic muscles is active clothing, i.e. garments with integrated PAMs used for rehabilitation purposes or to assist the movement of the upper or lower limbs of the human body [23].
This article introduces textile pneumatic muscles entirely designed at the Politecnico di Torino Department of Mechanical and Aerospace Engineering (DIMEAS). The textile structure, with interior latex, was chosen because its light weight, low bulk, comfort, fit and biocompatibility make it suitable for biomedical applications in active suits.
Textile materials are characterized by a distinct hierarchy of structure, which should be represented by a model of textile geometry and mechanical behaviour [15-22].

2 DIMEAS TEXTILE PNEUMATIC MUSCLE PROTOTYPE

The muscle prototype consists of: two end fittings (Figure 1), one at the front which is perforated to allow air to be supplied to the muscle, and one at the rear which acts as a plug; one layer of fabric; and one layer of latex. Cone sealing couplings are used to secure the double fabric-latex

ISSN 1590-8844
International Journal of Mechanics and Control, Vol. 17, No. 01, 2016

layer at the two ends. The fabric used is anisotropic and not airtight.
In particular the internal latex tube increase the size of structure but it avoids air loss from seam. The textile structure gives to the muscle stiffness and robustness. Furthermore it has a proper wearability for active suits. The tissue choice has to consider the maximum contraction obtainable and a proper load sustaining capacity.
In this paper cylindrical end-fitting of the muscle are used only for these preliminary experimental tests, while for an active suits a rectangular end-fitting of the muscle is preferable in order to improve wearability.
The wide study on various anisotropic fabrics carried on is useful for the choice of an anisotropic tissue with a proper radial elasticity and a good axial contraction. This study looks for a light and comfortable tissue, capable of working for a lot of cycles without any damage.
In particular Figure 2 shows an initial prototype of active suit fully developed and constructed in DIMEAS. It is made of a T-shirt with some DIMEAS textile pneumatic muscles prototypes put on the arm.
The initial experimentation on this prototype is still in progress and it is giving good results.

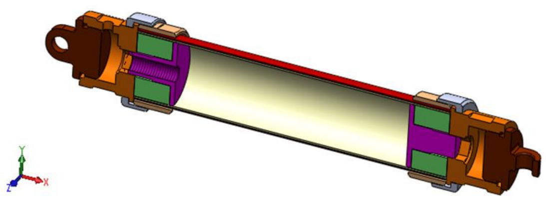

a)

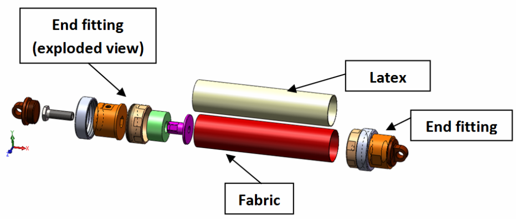

b)

Figure 1 a) Pneumatic muscle with textile structure, b) Exploded view of muscle.

Figure 2 A preliminary DIMEAS prototype of active suits.

3 WORKING METHOD

Tests were conducted on a tensile testing machine to evaluate the mechanical properties of the fabric and the latex used.
Testing was performed in accordance with ISO 13934-1 - Part 1: "Textiles - Tensile properties of fabrics - Determination of maximum force and elongation at maximum force using the strip method" [24], and ISO 13934-2 - Part 2: "Textiles - Tensile properties of fabrics - Determination of maximum force using the grab method" [25].
Subsequently, pressure-contraction and pressure-force tests were conducted on a sensorised test bench built specifically for this purpose.
Lastly, preliminary models were developed to simulate the prototypes' operation and investigate their behaviour.
The numerical models realised are: isotropic, anisotropic with fabric only, anisotropic with separate layers of latex and fabric, anisotropic with a single equivalent latex-fabric layer, anisotropic single equivalent layer with modified joint, anisotropic single equivalent layer with imposed elongation (model 6). As the model 6 is the best of the all models realized, only this last one is here presented.

4 EXPERIMENTAL TESTS

The experimental tests here presented were carried on both using a standardized test material machine and an experimental muscle test bench. Referred to the experimental results here presented it is underlined that 1 bar = 10^5 Pa.

4.1 MATERIAL CHARACTERIZATION

To gain an understanding of certain characteristics of the materials, fabrics were tested in tension [14, 26, 27] according to the standards indicated above and using a standardized test machine.
In particular various kind of tests with various tissue were carried on in order to measure elastic modulus of the samples.
The fabric specimen is secured between a stationary lower clamp and a moving upper clamp. The total stroke of the crossbar is about 1.5 meters. A load cell is connected to the upper clamp and the crossbar to measure the forces acting on the specimen and transfer them to a special software program. Tests were carried out using a pull rate of 2 mm/s.
Using the standardized test machine, 102 experimental tests were carried on with specimens geometry in full agreement with standards [14, 26, 27] and made of various fabrics.
Base on the comparative analysis shown in Table I, where the various parameters are: El elastic direction; R rigid direction; the tensile strength σ_e (the upper limit of elastic deformation regime); the shear stress σ_r (the rupture stress); the elastic strain ε_e and the rupture strain ε_r, it is possible to conclude that:

- the Fabric A is a material in which the stress does not overcome 0.8 N/mm^2 and it has a transpiring membrane that does not give air impermeability criteria;

- the Fabric B has an elastic structure and an permeable to air membrane which is extremely sensitive to high stresses and for this reason is not suitable for this study;
- the Fabric C is a resistant material with an impermeable membrane. It detaches itself from the textile layer and so the material integrity is no longer preserved;
- the Fabric D is an optimum material but the membrane is transpiring that do not respect the air impermeability condition;
- the Fabric E has good mechanical property and air impermeability and for those reasons this material is suitable for manufacturing process of the textile PAM's here presented.

Tests were performed in two directions (elastic and rigid) to characterize the material anisotropic behaviour. Specimens measure 200 x 50 mm as required by the standard in all tests, carried out here referred in particular to Fabric D and Fabric E as the best fabrics examined.
Fabric D consists of woven warp and filling yarns, while Fabric E is a knit, i.e. continuous interlocking loops produced from a single yarn. Fabrics have various layers: an inner transparent polyurethane membrane and outer polyester layers.
For each type of material, the test was repeated several times using three different specimens.

Table I - The comparative analyse of laminated fabric tested.

Material /Direction		σ_e [N/mm^2]	ε_e [%]	σ_r [N/mm^2]	ε_r [%]	E [N/mm^2]	Notes
FABRIC A Bi-laminate	-	1	40	6.4	81	4	- Fatigue resistance to external loads between 40 – 80 N; - Transpiring membrane and sensible to gripping device; - Permanent plastic deformations;
FABRIC B Bi-laminate	El	2	60	8.3	120	2.5	- Fatigue resistance to external loads between 50 – 100 N; - Membrane that detaches from the textile layer; - Permanent plastic deformations - Are proposed further investigations for lower external loading.
	R	16	31	17	33	50	- Fatigue resistance to external loads between 300 – 400 N; - Membrane that detaches from the textile layer ; - Permanent plastic deformations.
FABRIC C Tri-laminate	-	2.5	5	27	25	-	- Fatigue resistance to external loads between 400 – 600 N; - Transpiring membrane; - Permanent plastic deformations.
FABRIC D bi-laminate	El	0.8	35	6.8	71	1.2	- Fatigue resistance to external loads between 100 – 150 N; - Transpiring membrane and sensible to gripping device; - Permanent plastic deformations.
	R	1	3	21	25	-	- Fatigue resistance to external loads between 100 – 250 N; - Transpiring membrane and sensible to gripping device; - Permanent plastic deformations.
FABRIC E Tri-laminate	El	1	80	2.5	117	0.6	- Fatigue resistance to external loads between 20 – 40 N; - Permanent plastic deformations.
	R	2	30	18	68	5	- Fatigue resistance to external loads between 100 – 300 N; - Permanent plastic deformations.

Selected tensile test results for Fabric D are shown in Figure 3, where elongation is plotted on the abscissa and the force on the specimen during the tensile test is plotted on the ordinate. In this graph the specimens tested are both in textile material (in its rigid and elastic direction respectively) and in tissue and latex rubber linked together, in order to measure the elastic modulus of a sample made of two different materials. This is important as the pneumatic muscle structure here considered is made of textile material and latex rubber internal tube.

For each case, consecutive tests were performed, with results showing good repeatability.

For clarity, only the average curves from the various tests are given in the figure.

The tests start with the specimen in the initial unreformed condition (200 x 50 mm).

The initial cross sectional area of the fabric layer is 15 mm^2.

As can be seen from the graph in Figure 3 (Fabric D), only the latex and fabric specimen tested in the tissue elastic direction shows good linear behaviour, while the other cases show nonlinearities related to the materials employed.

The curves for the elastic fabric with latex sample and the rigid fabric with latex sample were used to calculate the elastic modulus according to ISO 527-1/2, 2012 [28, 29]; ISO 527-3, 1995 [30]; ISO 527-4, 1997 [31]; ISO 527-5, 2009 [32], given a specimen section of 15 mm^2.

Two values were obtained: 14106 Pa for latex rubber + tissue in elastic direction, and 122106 Pa for latex rubber + tissue in rigid direction.

These values were then used to model the muscles under examination.

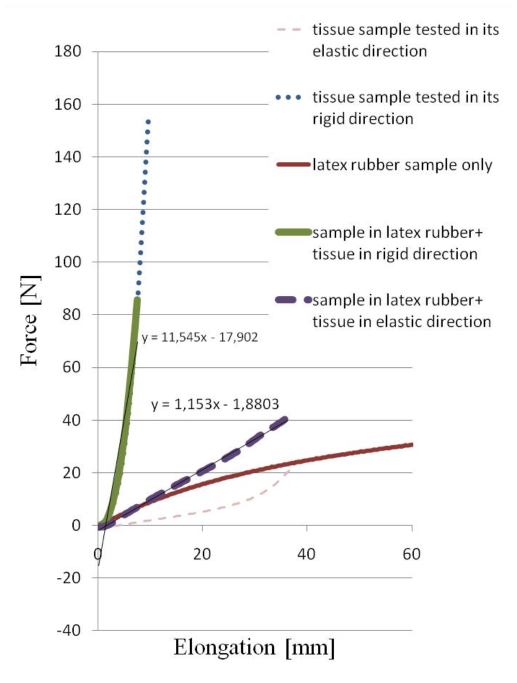

Figure 3 Tensile force versus longitudinal elongation (Fabric D).

Figures 4a and b show the Fabric E with latex behaviour during the tests in the elastic direction and in the rigid direction, showing here the only interpolation curves. From these tests the elastic module E is obtained both in the elastic direction (E_y = 3544426 N/m^2) and in the rigid direction (E_x = 14146596 N/m^2).

Given that the pneumatic muscle is a cylindrical structure with a sewn seam in the fabric, specimens featuring different types of seam were constructed in order to gain a better understanding of the fabric tensile behaviour.

Another possibility for joining the fabric could be hot welding. This type of method was studied in earlier stage of the research project of pneumatic muscles and turned out not to be successful. A problem was the increase of rigidity in the joining points, which is a result of melted fabric. To maintain elasticity in one direction is vital for the pneumatic muscles. Joining the fabrics with glue has also been tested, that turned out not to be successful.

The seam shall preferably have characteristics so that it rather supports the essential fabric properties, for the muscles performance, than impair them.

The seam shall have rigid properties, preferably as similar as possible to the ones of the fabric. Likewise shall the seam support the elasticity in the seam direction of the elongations muscles. Therefore the knowledge of the seam behaviour in the fabric is necessary.

Tests were performed accordingly on the fabric with seam/seams to determine the seams impact in the fabric regarding the rigidity verses elasticity.

Three samples were performed in the same way on the same machine, the MTS-machine.

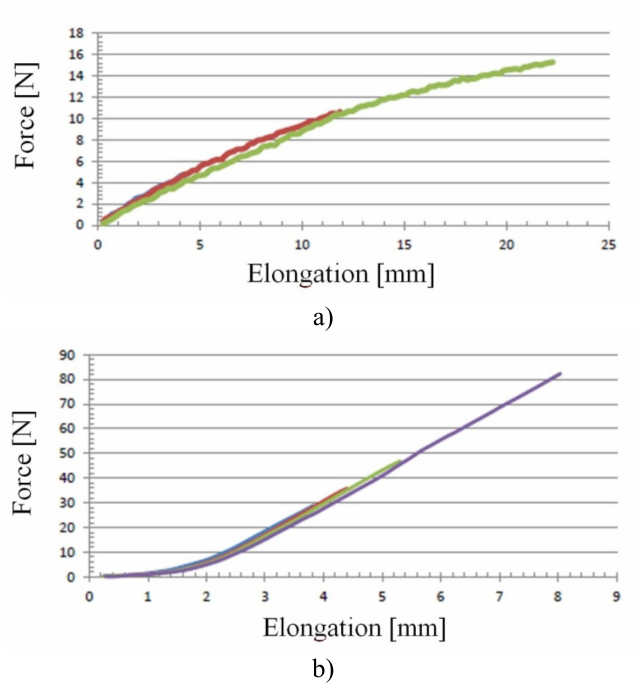

Figure 4 a) Fabric E, elastic direction: Load-Elongation tensile test curve; b) Fabric E, rigid direction: Load-Elongation tensile test curve.

Because of unidirectionality of the MTS-machine was the behaviour of muscle in each direction, longitudinal and radial, studied separately. Each direction was studied for both types of muscles that are elastic and rigid direction. This analysis was focused on the effect of the seam in the longitudinal direction of the muscle. Some of the results obtained on Fabric D and Fabric E are shown in Table II.
The first column indicates whether or not the specimen features a seam, the second column shows the maximum force allowable for a proper use of the material, the third indicates the corresponding elongation, the fourth indicates the contribution of a single seam in the case of specimens with four seams to evaluate their effect on the specimen elongation under a maximum allowable force value.
In addition, the table summarizes the force and elongation values recorded during tests along the elastic and rigid directions. Comparing the two tissues it can be noticed a similar behaviour on both fabrics.
To work in the elastic area of the fabric is important in order to avoid a damage of the muscle structure during its functioning. Furthermore several other fabrics were tested with and without seams of various kinds, in order to carry out a detailed analysis of the characteristics of possible materials useful for in the construction of pneumatic muscles.

Table II – Tensile tests on Fabrics D and E.

<table>
<tr><td colspan="2">FABRIC D</td><td colspan="2">MAXIMUM FORCE RANGE [N]</td><td>ELONGATION RANGE [mm]</td></tr>
<tr><td colspan="2">Elastic direction (El)</td><td colspan="2">10-15</td><td>9-28</td></tr>
<tr><td colspan="2">Rigid direction (R)</td><td colspan="2">35-60</td><td>4.0-4.8</td></tr>
<tr><td>FABRIC D</td><td colspan="2">Average maximum allowable force [N]</td><td>Elongation [mm]</td><td>Contribution of one seam [mm]</td></tr>
<tr><td>Without seams (El)</td><td colspan="2">14</td><td>28</td><td>-</td></tr>
<tr><td>With seams (El)</td><td colspan="2">16</td><td>9-15</td><td>15-20</td></tr>
<tr><td>Without seams (R)</td><td colspan="2">50</td><td>4.2</td><td>-</td></tr>
<tr><td>With seams (R)</td><td colspan="2">60</td><td>4.3</td><td>4.2</td></tr>
<tr><td colspan="2">FABRIC E</td><td colspan="2">MAXIMUM FORCE RANGE [N]</td><td>ELONGATION RANGE [mm]</td></tr>
<tr><td colspan="2">Elastic direction (El)</td><td colspan="2">4-15</td><td>4-15</td></tr>
<tr><td colspan="2">Rigid direction (R)</td><td colspan="2">40-60</td><td>3.3-4.5</td></tr>
<tr><td>FABRIC E</td><td colspan="2">Average maximum allowable force [N]</td><td>Elongation [mm]</td><td>Contribution of one seam [mm]</td></tr>
<tr><td>Without seams (El)</td><td colspan="2">13</td><td>15</td><td>-</td></tr>
<tr><td>With seams (El)</td><td colspan="2">20</td><td>4-9</td><td>12-14</td></tr>
<tr><td>Without seams (R)</td><td colspan="2">50</td><td>3.7</td><td>-</td></tr>
<tr><td>With seams (R)</td><td colspan="2">50</td><td>1.5-4.5</td><td>3.4-4.4</td></tr>
</table>

4.2 TESTS ON PNEUMATIC MUSCLE PROTOTYPES

The experimental muscle test bench constructed at the Politecnico di Torino DIMEAS laboratory to validate prototype pneumatic muscles is pictured in Figure 5.

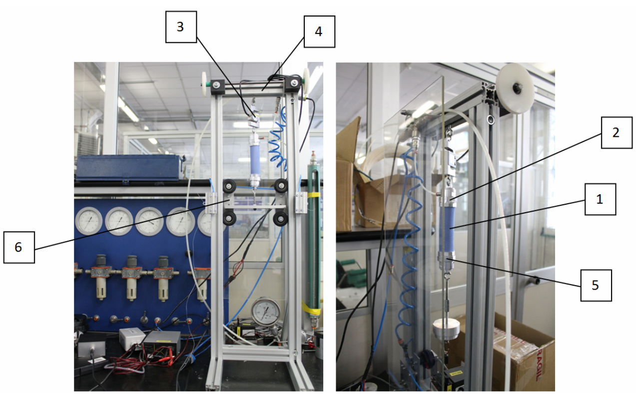

Figure 5 Muscle test bench.

The muscle (1) is mounted vertically with the rigid fabric direction along the muscle axis and its front end fitting (2) is attached to a load cell (3) connected directly to the fixed frame (4). The muscle's rear end fitting (5) has a threaded hole to receive the end of a flush position transducer and a lower crossbar (6) which slides vertically and can be attached to weights.
To minimise friction, the mobile crossbar is mounted on rollers with a guide that facilitates vertical motion.
Using the muscle prototypes test bench here presented various kinds of cylindrical muscles were tested, with diameters variable from 13 mm to 30 mm and length at rest 100 mm, built with Fabric D and E.
Muscle supply pressure is adjusted manually via a pressure reducer from 0 to 1.5 relative bar. To measure the force that the prototype is able to exert at a certain set length, the mobile crossbar can be locked on the frame.
The software records muscle pressure, stroke and pulling force. Data are acquired at a sampling frequency of 5 Hz, i.e. one sample every 200 ms.

ISSN 1590-8844
International Journal of Mechanics and Control, Vol. 17, No. 01, 2016

The initial length of the pneumatic muscle under test is 100 mm.
For the sake of brevity, only certain selected muscle pressure-contraction and hysteresis tests are shown, as these are the tests that are most useful for comparison with the next model that was developed.
Furthermore in some fabrics here tested an initial assessment of material was noticed.
Anyway after this phenomenon all of materials work without any plastic deformation or damage.
In the Figures 6a and 7 some experimental graphs obtained using Fabric D and Fabric E are illustrated.
It is possible to notice that Fabric D shows a lower load capacity and less contraction, due to its different anisotropic textile structure, as radial deformation and axial contraction.
In Figure 6a, muscle M_1 contraction is plotted versus supply pressure, with a load consisting of the mobile crossbar alone (1 kg) and, for a closer examination of the muscle behaviour, with an additional 5 kg external load.
The muscle M_1 has the structure shown in Figure 1.
The percentage contraction shown in the graph in Figure 6a was calculated with the formula:

$$Contraction\% = 100\frac{L_0 - L_f}{L_0} \tag{1}$$

where L_0 = initial length, L_f = final length of the muscle tested.

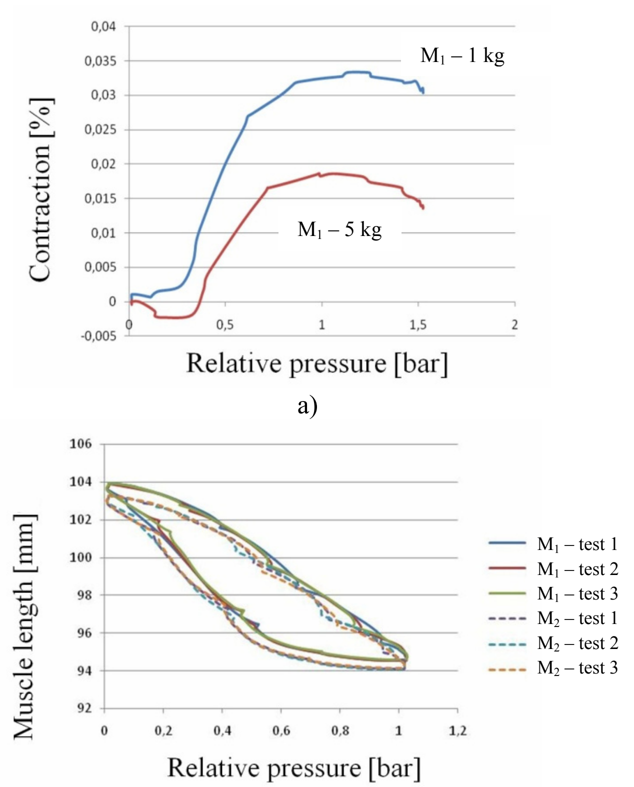

a)

b)

Figure 6 a) Examples of experimental tests on muscles with Fabric D and inner latex tube; b) Hysteresis tests on the materials used (p_{max} = bar; load 5 kg – Fabric D).

Given their structure, the muscles also present hysteresis.
Their active and passive strokes do not coincide, and this hysteresis is due to friction phenomena both between the inner latex layer and the outer fabric, and between the fabric's weft and filling yarns.
In particular, Figure 6b illustrates the hysteresis cycle in two pneumatic muscles (M_1 and M_2) of the same geometry subjected to an external load of 5 kg. The muscles M_1 and M_2 have the structure shown in Figure 1.
A hysteresis cycle is clearly present for both prototypes m1 and m2 in three consecutive trials.
As can be seen from the graph, results show good repeatability for both muscles.
Using Fabric E also a different muscle structure was experimented, as shown in Figure 7 where the prototypes behaviour of new different muscles (called M_a-M_b-M_c-M_d) are shown.
In fact with Fabric E only the Ma muscle prototype (Figure 7) was constructed with the same structure used for Fabric D here shown in Figure 1.
The other prototypes presented in Figure 7 instead were built with some axial wires connected between the two muscle end-fittings in order to increase the textile load capacity.
In Figure 7 experimental tests with fabric E are shown, using the formula (1) for the percentage contraction calculation. These tests were carried out on pneumatic muscles with 30 mm nominal diameter and 100 mm length, varying supply pressure from 0.5 bar to 1.5 bar without any external load applied to the muscle.
In particular the best performance was obtained with the prototype M_a, comparable with the structure of the muscle above described with fabric D.
This demonstrate that the addition of axial wires does not improve the characteristics of the muscle that also with Fabric E works better with design illustrated in Figure 1.

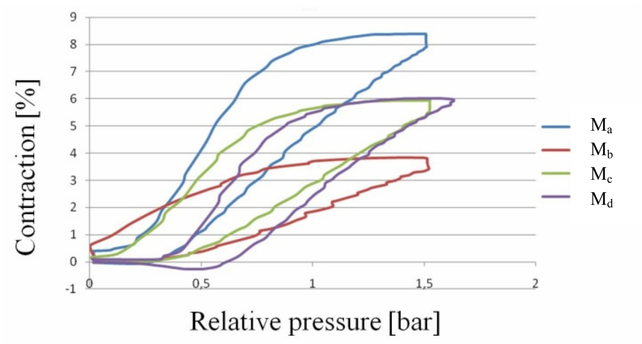

Figure 7 Examples of experimental tests on muscles with Fabric E and inner latex tube.

5 MUSCLE NUMERICAL MODELS

Several initial models were constructed which can be useful in developing a rapid and reliable method for designing and validating these pneumatic muscles and for modelling their application in an active suit in order to study in the future the optimal linkage and geometry muscle configuration for this purpose.

In particular, model 6 refers to simulations of an entire muscle assembly consisting of an outer fabric sheath and an inner latex tube.

The assumption of a linear elastic material made here is compatible with the fact that the muscle's contraction is here very limited (about 3 mm out of a length at rest of 100 mm), as was determined in the experimental tests.

For the present purposes, the nonlinearity of the material used can thus be neglected.

The hysteresis shown by the tested prototypes does not affect the initial models presented as they simulate a unidirectional, non-cyclic movement.

The elastic modulus and Poisson's ratio used initially for the models were those provided directly by the MTS tensile testing machine on hybrid fabric + latex samples.

As regards the orthogonal reference system, the x axis is along the muscle axis, while axes y and z are radial.

In the present case, the muscle model is constrained at the rear end fitting, while the front end fitting is free to move axially. All simulations presented refer to muscles of 100 mm length and 30 mm outside diameter, with different models constructed as seamless cylinders. No external load was applied to the muscle at this stage of the investigation.

The air pressure used in the models is 0.2-0.5-1.0 relative bar.

The software calculates stresses, elongations and strains.

For each point, there are three mutually orthogonal planes, called the principal stress planes, with normal vectors (σ_1, σ_2, σ_3) as the principal stress directions. The main stresses here used are σ_x, σ_y, σ_z located according to the [x, y, z] reference system used in the models, as are the three tangential components τ_{xy}, τ_{xz}, τ_{yz}.

The optimal model that was developed (model 6) is presented below.

As the material is anisotropic material, it was not possible to use the Von Mises yield criterion. According, the Hashin failure criterion [33, 34] was considered, as it is suitable for anisotropic composite materials. This criterion defines an interaction between the normal stress and the shear stress.

5.1 ANISOTROPIC MODEL WITH A SINGLE EQUIVALENT LAYER AND INTERLOCKING MODIFIED AS IMPOSED ELONGATION

The substantial limit of the simulations carried out with the first models lies in the areas of maximum fabric strain near the end fittings. In those areas, the radial preload to which the fabric is subjected when the muscle is attached to the cone sealing couplings was neglected.

In model 6, a 0.7 mm fictitious radial elongation is imposed in the two end sections of the tube in order to simulate the fabric prestress resulting from the actual assembly method.

In these conditions, a circumferential tensile stress state is generated which initially decreases when the internal pressure increases. The assumptions made are: linear elastic materials; only one equivalent material, homogeneous and anisotropic (equivalent elastic modulus E obtained from experimental tests on the hybrid specimens); elongation imposed on the ends to simulate the assembly prestress; one of the two ends of the muscle constrained, as otherwise the structure would be unstable; none external load applied to the muscle during simulation. The Hashin criterion is used to verify yield strength.

5.2 ANALYSIS OF RESULTS

The actual geometry of the end fitting is shown in Figure 8a, where the prestressed area of the fabric is circled in blue. Prestressing is obtained by imposing a 0.7 mm radial elongation over an axial length of 17 mm on both ends of the cylinder that simulates the pneumatic muscle under examination. Figures 8b and 8c illustrate the Von Mises equivalent stress along the muscle x axis, simulated with this model supplied at 0.5 relative bar. The strain is now consistent with the experimental results, and the contraction along the x axis is 3.2 mm (Fabric D). Figure 8c shows a detail of the Von Mises stresses calculated in the area of the elongation (supply pressure = 0.5 relative bar). Figures 8d and 8e show the axial contraction of the muscle modelled here, again with a supply pressure of 0.5 relative bar. A modelled muscle contraction detail along the x axis is plotted in Figure 8e.

Also in this case, yield strength checks on the data obtained from the model were made using Hashin's formula with a supply pressure of 0.5 relative bar and 1 relative bar.

The calculations made with Hashin's formula indicate that the muscle will not fail when subjected to a supply pressure of 0.5 relative bar, but that failure will take place at 1 relative bar.

In particular, in analyzing the actual samples, the fabric remains unchanged and adheres to the inner latex tube with the 0.5 relative bar supply pressure.

During experimental tests at 1 relative bar, the fabric is altered and a residual strain persists.

The contraction obtained with numerical model 6 in these conditions is 3.2 mm, while the experimental contraction is 3 mm at a relative supply pressure of 0.5 relative bar.

The error between the model and the experimental result is therefore 6.7 % with 0.5 relative bar supply pressure.

Given the assumptions made and the parameters included in the model, it can be concluded the model provides good results in this case.

At a supply pressure of 1 relative bar, by contrast, failure occurs when numerical model 6 is used with Hashin's formula. Alterations in the pneumatic muscles' outer fabric sheath also occurred at this pressure in the experimental tests. In this case, the error between the model and the experimental result is -36.4 %.

Since the discrepancies between the theoretical model and the data measured on the prototypes may also be due to the experimental values of Young's modulus, a sensitivity analysis of the two Young's moduli used in model 6 was performed, starting from the data provided by the standardized test machine software.

This analysis consists in varying one parameter at a time, moving in the plane illustrated in Figure 9.

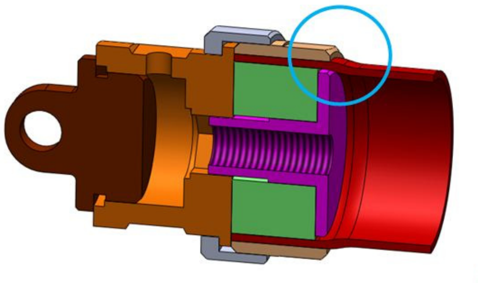

a)

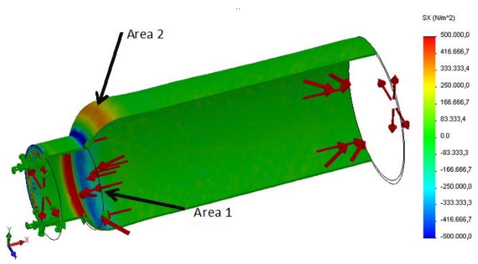

b)

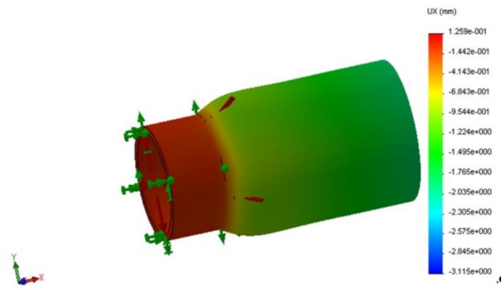

d)

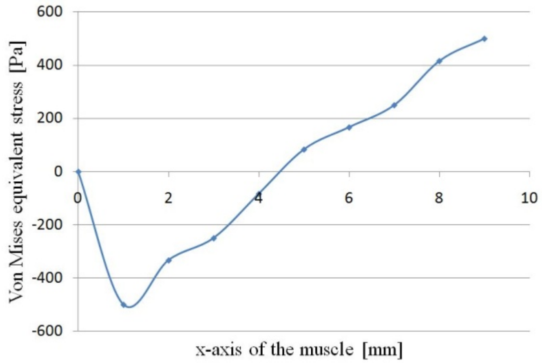

c)

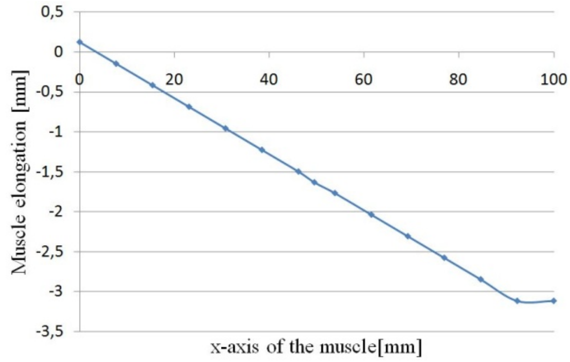

e)

Figure 8 a) Details of the actual muscle end fitting
b) c) Normal stress σ_x in the cone sealing attachment area
d) Detail of the area with sharp edge
e) Axial strains (x) of the muscle over the entire length (100 mm).

Each point, designated with a letter, represents the increments to the initial values of the moduli with a variation of 10 %.

In all analysis presented here, the supply pressure was considered to be 1 relative bar and the load was 1 kg.

This is useful in order to evaluate the muscle's performance at supply pressures sufficient to move the human upper limb correctly when the muscle prototype is integrated in active clothing used for rehabilitation exercises or as an aid for the disabled.

Twelve simulations were then performed on the basis of the twelve points represented above.

The contraction values and the percentage error for model 6 are shown in Table III and compared with the experimental results.

The error between the contraction values obtained with the model and with the experimental tests was also calculated using the formula:

$$Err_{\%} = 100\frac{Contraction\%_{Exp} - Contraction\%_{Mod}}{Contraction\%_{Exp}} \qquad (2)$$

The negative percentage errors indicate that pneumatic muscle model 6 overestimates the experimental results, while positive percentage errors indicate that model 6 underestimates the experimental results.

As can be seen from Table III, the best pair of increments in Young's modulus is provided by point L, at which there is a 15 % increase in Young's modulus along the x direction

and 10 % along the y axis.
This also helps balance out any approximations related to the use of Hashin's criterion for knitted fabrics.
A comparison of the results of this sensitivity analysis with the elastic modulus E calculated according to (ISO 527-1/2, 2012; ISO 527-3, 1995; ISO 527-4, 1997; ISO 527-5, 2009) [30-34] from the experimental data shown in Figure 3, i.e. 14106 Pa for the latex + elastic specimen, shows good agreement.
In particular, it should be noted that the sensitivity analysis presented here was very useful, inasmuch as the elastic modulus data provided by the tensile testing machine software show uncertainties related to the hybrid structure of the specimens.
In fact, the tested materials consist of two parts (latex rubber + tissue sample), and the fabric consists of woven yarns, and is thus more complex than a homogeneous material.

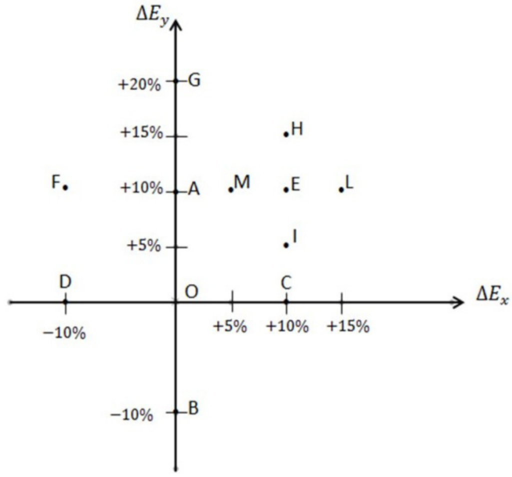

Figure 9 Sensitivity analysis.

Table III – Contraction analysis with Fabric D.

Point	$E_x + \Delta E_y$ [Pa]	$E_y + \Delta E_x$ [Pa]	Simulation contraction [mm]	Experimental contraction [mm]	Percentage error [%]
O	11873108	1806514	3	2.2	-36.4
A	11873108	1987165	2.8	2.2	-27.3
B	11873108	1625863	3	2.2	-36.4
C	13060419	1806514	2.8	2.2	-27.3
D	10685797	1806514	3.2	2.2	-45.4
E	13060419	1987165	2.6	2.2	-18.2
F	10685797	1987165	3	2.2	-36.4
G	11873108	2167817	3.4	2.2	-54.5
H	13060419	2077491	2.9	2.2	-31.8
I	13060419	1896840	2.7	2.2	-22.7
L	**13654074**	**1987165**	**2.5**	**2.2**	**-13.6**
M	12466763	1987165	2.7	2.2	-22.7

In Figure 10 results obtained with model 6 and Fabric E are shown, referred to the experimental results shown in Figure 7.
In the model the muscle (length 100 mm, diameter 30 mm) has an extremity fully fixed and the other one capable of moving axially, with a contraction equal to 6.6 mm.
With Fabric E the calculation of E modulus was been carried on as here explained.
To calculate stress σ_s and Young's modulus E, yielding force F_s and sample elongation were measured, in order to use the formula $\sigma_s = F_s / A$ with A = wide*thickness of the sample.
In this way, using the formula

$$p_{\lim} = \frac{2\ F_s}{d\ L} \quad (3)$$

it is possible to calculate the maximum supply pressure ($p_{\lim}$) for the fabric without any damage in its structure.

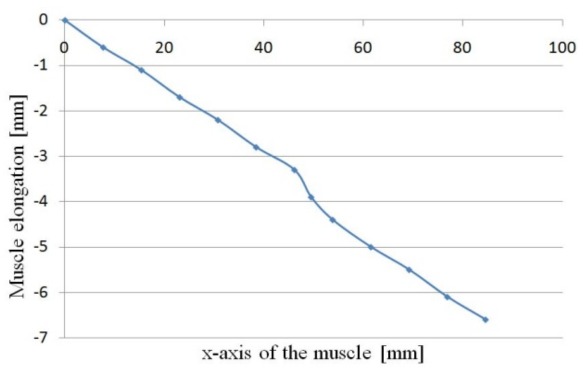

Figure 10 Axial strains (x) of the muscle over the entire length (100 mm – Fabric E).

In the formula d is the latex tube internal diameter and L is the sample wide. Fabric E has a higher contraction than Fabric D both in the simulation and in the experimental tests. In Table IV the results obtained from simulation and the percentage error between experimental and numerical results are shown using Fabric E and various supply pressure. In particular: in the first simulation an anisotropic material was imposed with $E_x = 6845153$ N/m^2, $E_y = 3544426$ N/m^2, Poisson's ratio $\nu_{xy} = 0.35$, $\nu_{yz} = 0.32$, $\nu_{xz} = 0.32$; in the second simulation an anisotropic material was created with $E_x = 6845153$ N/m^2; E_y variable with the supply pressure applied, $E_z = 14146596$ N/m^2, Poisson's ratio variable; in the third simulation an anisotropic material equal to the second simulation was imposed with Poisson's ratio equal to $\nu_{xy} = 0.31$, $\nu_{yz} = 0.28$, $\nu_{xz} = 0.28$; in the forth simulation $E_x = 6845153$ N/m^2, $E_y = 3544426$ N/m^2, E_z and Poisson's ratio variable with the supply pressure applied were used. Overall the best correspondence between experimental and numerical model results is obtained with the first-second-third simulation.

Table IV – Contraction analysis with Fabric E.

Pressure [bar]	Contraction [mm] and percentage error					
	Experimental	Simulation1	Simulation2	Simulation3	Simulation4	Simulation5
0,5	**1,3**	2,3	2,3	1,9	3,1	3,0
		-76,92 %	-76,92 %	-46,15 %	-138,46 %	-130,77 %
0,8	**3,4**	3,6	3,8	3,4	5,0	5,4
		-5,88 %	-11,76 %	0,00 %	-47,06 %	-58,82 %
1	**5,0**	4,5	5,4	4,9	6,2	7,8
		10,00 %	-8,00 %	2,00 %	-24,00 %	-56,00 %
1,3	**7,1**	5,9	8,6	8,3	7,9	11,9
		16,90 %	-21,13 %	-16,90 %	-11,27 %	-67,61 %
1,5	**8,4**	6,9	10,9	10,9	8,8	14,3
		17,86 %	-29,76 %	-29,76 %	-4,76 %	-70,24 %

6 CONCLUSIONS

This article presents a preliminary study of several prototype pneumatic artificial muscles that can develop tensile forces when supply pressure is varied, and which consist of a textile structure. Their applications, in this case, are in the biomedical field, i.e. in rehabilitation and in assisting upper limb movement. Experimental tests were carried out to characterize the materials used and to gain an understanding of each prototype performance. These tests were followed by a theoretical study. The theoretical models of muscles presented here are reliable, as they relate to a muscle contraction which is small enough to be regarded as within the range of linear behaviour. The results obtained are good and provide interesting ideas for further work on these prototypes. In the next stage of the study presented here, the performance of the preliminary prototypes will be optimised in terms of achievable axial contraction. Now new experimental tests are carried on using a stronger textile material, directly produced on the market with a cylindrical geometry. This avoid the seam presence in the muscle prototype. Anyway the latex internal tube is required in order to guarantee the system air tightness.

ACKNOWLEDGEMENTS

Authors thanks Eng. A.L. Visan, Eng. F. Ekholm, Eng. C. Keipert, Eng. E. Rulfi, Eng. D. Contigiani for their help in this research.

REFERENCES

[1] Ranjan R., Upadhyay P. K., Kumar A. and Dhyani P., Theoretical and experimental modeling of air muscle. *International Journal of Emerging Technology and Advanced Engineering*, Vol. 2, No. 4, pp. 112-119, 2012.

[2] Wickramatunge K. C. and Leephakpreeda T., Empirical modeling of pneumatic artificial muscle. *Proceedings of the International MultiConference of Engineers and Computer Scientists*, Hong Kong, II, 2009.

[3] Pilch Z. and Bieniek T., Pneumatic muscle – measurement results and simulation models. *Proceedings of Electrotechnical Institute*, Issue 240, pp. 179-193, 2009.

[4] Belforte G., Quaglia G., Testore F., Eula G. and Appendino S., Wearable textiles for rehabilitation of disabled patients. *Smart Textiles for Medicine and Healthcare The Textile Institute*, Cambridge, UK In: L. Van Langenhove (Ed.), Chapter 12, pp. 221-251, 2007.

[5] Belforte G., Eula G. and Appendino S., Design and development of innovative textile pneumatic muscles. *The Journal of the Textile Institute*, doi: 10.1080/00405000.2011.603508, iFirst, pp. 1-11, 2011.

[6] Belforte G., Eula G., Ivanov A. and Visan A.L., Bellows textile muscle. *The Journal of the Textile Institute*, doi: 10.1080/00405000.2013.840414, Vol. 105, No. 3, pp. 1-9, 2014.

[7] Belforte G., Eula G., Ivanov A., Grassi R., Askri H. and Appendino S., Comparison of assembly techniques for textiles used in pneumatic devices. *The Journal of the Textile Institute*, doi: 10.1080/00405000.2013.846494, Vol. 105, No. 7, pp. 717-728, 2014.

[8] Belforte G., Eula G., Ivanov A. and Sirolli S., Soft pneumatic actuators for rehabilitation. *Special Issue "Soft Actuators" - Actuators*, doi: 10.3390/act3020084, Vol. 3, pp. 84-106, 2014.

[9] Ching-Ping C. and Blake H., Measurement and modeling of McKibben pneumatic artificial muscles. *IEEE Transactions on Robotics and Automation*, Vol. 12, No. 1, pp. 90-102, 1996.

[10] Klute G.K., Czerniecki J.M. and Hannaford B., McKibben Artificial Muscles: Pneumatic Actuators with Biomechanical Intelligence, IEEE/ASME 1999 Int. Conference on Advanced Intelligent Mechatronics (AIM ’99), Atlanta (GA), 1999.

[11] Lomov S.V., Huysmans G., Luo Y., Parnas R.S., Prodromou A., Verpoest I. and Phelan F.R., Textile composites: modelling strategies. *Composites*, *Part A*, Vol. 32, No. 10, pp. 1379-1394, 2001.

[12] Caldwell D.G., Medrano-Cerda G.A. and Bowler C. J., Investigation of bipedal robot locomotion using pneumatic muscle actuators. *Proceedings of the 1997 IEEE International Conference on Robotics and Automation*, Albuquerque, New Mexico, 1997.

[13] Kobayashi H. and Hiramatsu K., Development of muscle suit for upper limb. *Proceedings of the 2004 IEEE International Conference on Robotics and Automation*, New Orleans, LA. 2004.

[14] Pan N. and Yoon M.Y., Structural anisotropy, failure criterion, and shear strength of woven fabrics. *Textile Res. J.*, doi: 10.1177/004051759606600409, Vol. 66, No. 4, pp. 238-244, 1996.

[15] Visan A., Alexandrescu N., Belforte G., Eula G. and Ivanov A., Experimental researches on textile laminate materials, *Industria Textila*, Vol. 63, No. 6, pp. 315-321, 2012.

[16] Boržíková J., Balara M. and Pitel J., The mathematical model of contraction characteristic k = (F,p) of the pneumatic artificial muscle. *Proceedings of XXXII. Seminar ASR'2007 - Instruments and Control*. pp. 21-25, 2007.

[17] Doumit M., Fahim A. and Munro M., Analytical modelling and experimental validation of the braided pneumatic muscle. *IEEE Transactions on Robotics*, doi: 10.1109/TRO.2009.2032959, Vol. 25, No. 6, pp. 1282-1293, 2009.

[18] Manuello Bertetto A. and Ruggiu M., Characterization and modeling of air muscles. *Mechanics Research Communications*, doi: 10.1016/S0093-6413(03)00088 -0, Vol. 31, No. 2, pp. 185-194, 2004.

[19] Sui L. and Xie S., Modelling of pneumatic muscle actuator and antagonistic joint using linearised parameters. *Int. J. Biomechatronics and Biomedical Robotics*, pp. 67-74, 2013.

[20] Wang G., Wereley N.M. and Pillsbury P., Non-linear quasi-static model of pneumatic artificial muscle actuators. *Journal of Intelligent Material Systems and Structures*, doi: 10.1177/1045389X14533430, Vol. 26, No. 5, 2014.

[21] Kobayashi H., Hasegawa S. and Nozaki H., Development of muscle suit for supporting manual worker. *SICE Annual Conference 2007*, Kagawa University, Japan, 2007.

[22] Prior S.D. and White A.S., Measurements and simulation of a pneumatic muscle actuator for a rehabilitation robot. *Simulation Practice and Theory*, doi: 10.1016/0928-4869(95)00010-Q., Vol. 3, pp. 81-117, 1995.

[23] Sasaki D., Noritsugu T. and Takaiwa M., Development of wearable master-slave training device for upper limb constructed with pneumatic artificial muscles. *Proceedings of the 8th JFPS International Symposium on Fluid Power*, Okinawa, 2011.

[24] International Standard ISO 13934-1 (1999). *Textiles – Tensile properties of fabrics – Part 1: Determination of maximum force and elongation at maximum force using the strip method*.

[25] International Standard ISO 13934-2 (1999). *Textiles – Tensile properties of fabrics – Part 2: Determination of maximum force using the grab method*.

[26] Ekholm F., Textile pneumatic muscles design and testing for integration in textile active suits. E-team master’s thesis, Politecnico di Torino, Torino, Italy 2012.

[27] Keipert C., Design and testing of textile pneumatic muscles for rehabilitation devices. E-team master’s thesis, Politecnico di Torino, Torino, Italy 2012.

[28] Chen Q. and Pugno N.M., Modeling the elastic anisotropy of woven hierarchical tissues. *Composites*, doi: 10.1016/j.compositesb, Part B No. 42, pp. 2030-2037, 2011.

[29] Peng X.Q. and Cao J., A continuum mechanics-based non-orthogonal constitutive model for woven composite fabrics. *Composites*, Part A: Applied Science and Manufacturing, doi: 10.1016/j. compositesa.2004.08.008.2005; Vol. 36, No. 6, pp. 859-874, 2005.

[30] International Standard ISO 527-1:2012. *Plastics – Determination of tensile properties – Part 1: General principles*.

[31] International Standard ISO 527-2:2012 *Plastics – Determination of tensile properties – Part 2: Test conditions for moulding and extrusion plastics*.

[32] International Standard ISO 527-3:1995 *Plastics – Determination of tensile properties – Part 3: Test conditions for films and sheets*.

[33] International Standard ISO 527-4:1997 *Plastics – Determination of tensile properties – Part 4: Test conditions for isotropic and orthotropic fibre-reinforced plastic composites*.

[34] International Standard ISO 527-5:2009. *Plastics – Determination of tensile properties – Part 5: Test conditions for unidirectional fibre-reinforced plastic composites*.